Electronic effects in oxo transfer reactions catalysed by salan molybdenum(VI) *cis*-dioxo complexes†

Christopher J. Whiteoak, George J. P. Britovsek,* Vernon C. Gibson* and Andrew J. P. White

Received 21st November 2008, Accepted 9th January 2009
First published as an Advance Article on the web 17th February 2009
DOI: 10.1039/b820754b

A series of molybdenum(VI) *cis*-dioxo complexes containing tetradentate salan ligands with different *para*-substitutions on the phenoxy group have been prepared. These complexes catalyse the oxygen atom transfer reaction between dimethylsulfoxide and triphenylphosphine. During oxo transfer catalysis, the complexes are resistant to formation of catalytically inactive oxo-bridged dimeric Mo(V) complexes. Electronic effects influence the rate of the oxo transfer reaction and the fastest rates are achieved when the *para*-phenoxy substituent is an electron withdrawing nitro substituent. Hammett correlations have shown that the rate-determining step involves nucleophillic attack of the phosphine on one of the oxo ligands. Electrochemical measurements have shown that all complexes containing tertiary amine ligands exhibit quasi-reversible behaviour and that the *para*-substituent has a considerable effect on the half potentials ($E_{1/2}$). A linear correlation between the $E_{1/2}$ values and the Hammett σ_p parameter is observed.

Introduction

Enzymes containing molybdenum-based active sites for the oxidation of substrates *via* oxygen atom transfer reactions have been of interest for some time.[1–3] Three families of molybdenum enzymes have been identified: Sulfite Oxidase (SO), Dimethylsulfoxide Reductase (DMSOR) and Xanthine Oxidase (XO) and structural analyses of these enzymes have shown that all contain sulfur donors in the molybdenum coordination sphere. Understandably, most studies on model systems for these metallo-enzymes have used Mo and W complexes containing sulfur based ligands, in particular dithiolene ligands.[3–5] In addition, a number of non-dithiolene ligands have been investigated, including pyridine dithiolates,[6,7] tris(pyrazolyl)borate ligands,[8–13] β-ketiminates[14] and Schiff base ligands of the salen and salan type. The latter class of ligands were first investigated by Topich and Lyon, who prepared molybdenum complexes with tridentate Schiff base ligands and studied the oxo transfer properties of these complexes with phosphines.[15–18] Tetradentate salen and salan ligands and related ONNO and SNNS type ligands were employed by Enemark and co-workers[19–21] and the use of bulky substituents was investigated in order to prevent the formation of dimeric oxo-bridged Mo(V) complexes, which are generally considered the reason for catalyst deactivation in oxo transfer reactions.[22] More recently, Ng[23,24] and Lehtonen[25] have reported on the use of tetradentate salan ligands with amine and phenoxy donors. Specifically, Ng and co-workers[24] have shown that a tungsten dioxo complex with the salan ligand (*N*,*N*′-dimethyl-*N*,*N*′-*bis*[(2-hydroxyphenyl)methylene]-1,2-diaminoethane) [$WO_2(L^H)$] catalyses oxo-transfer reactions in the conversion of benzoin to benzil with dimethylsulfoxide (DMSO), which is a relatively reactive oxo transfer agent.[26] Lehtonen and Sillanpää have shown that the two molybdenum dioxo complexes with *ortho*/*para* substituted salan ligands [$MoO_2(L^{Me,Me})$] and [$MoO_2(L^{tBu,tBu})$] catalyse the oxo transfer reaction between DMSO and triphenylphosphine.[25] We were intrigued by these results and decided to investigate whether the reactivity of these molybdenum catalysts can be tuned such that, in future, other substrates may be oxidised with environmentally benign oxidants such as H_2O_2 or O_2.

We report here the synthesis and characterisation of an extensive series of molybdenum(VI) *cis*-dioxo complexes containing tetradentate salan ligands [$MoO_2(H_2L^H)$] and [$MoO_2(L^X)$] and a systematic study into the effect of the *para*-phenoxy substituent on the catalytic oxo transfer properties of these complexes (see Fig. 1). All complexes have been fully characterised and their catalytic

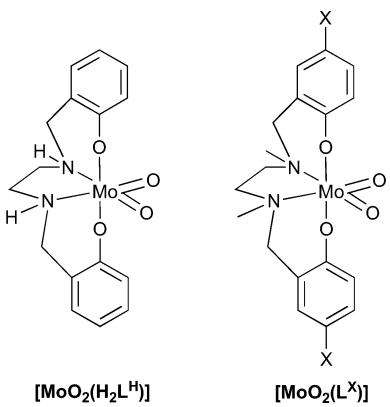

[$MoO_2(H_2L^H)$] **[$MoO_2(L^X)$]**

Fig. 1 Molybdenum dioxo salan complexes.

Department of Chemistry Imperial College London, Exhibition Road, South Kensington, London, UK SW7 2AY. E-mail: g.britovsek@imperial.ac.uk; Fax: +44 (0)20 75945804; Tel: +44(0)20 75945863

† Electronic supplementary information (ESI) available: further experimental data, cyclic voltammetry studies and Fig. S1. CCDC reference number 689173. For ESI and crystallographic data in CIF or other electronic format see DOI: 10.1039/b820754b

potential in oxo transfer reactions between DMSO and PPh_3 has been investigated. A detailed Hammett analysis has been carried out in order to investigate the correlation between the *para*-substituent and the reduction potential of these catalysts and with their catalytic activity.

Experimental

All syntheses of complexes were carried out using standard vacuum line, Schlenk, or cannular techniques or in a conventional nitrogen-filled glovebox. NMR spectra were collected on a Bruker DRX-400 spectrometer. Chemical shifts for ^{1}H and ^{13}C NMR are referenced to the residual protio impurity and to the ^{13}C NMR signal of the deuterated solvent. ^{19}F and ^{31}P chemical shifts are reported relative to $CFCl_3$ and H_3PO_4 (85%), respectively. Mass spectra were recorded on a VG Autospec spectrometer. Elemental analysis was performed by the Science Technical Support Unit at London Metropolitan University. Electrochemical studies were performed on an AD Instruments MacLab/2e utilising EChem software equipped with an Ag/AgCl reference, Pt wire counter and Pt stick working electrodes.

Solvents and reagents

Acetonitrile, dichloromethane and DMSO were dried by prolonged reflux over calcium hydride under a nitrogen atmosphere, being freshly distilled prior to use. *N*,*N*-dimethylformamide (DMF) and methanol was purchased dry from Sigma-Aldrich and stored over molecular sieves. All other reagents are commercially available and were used without further purification. $[MoO_2(acac)_2]$ was prepared according to a published procedure.[27] The ligands $\mathbf{H_4L^H}$, $\mathbf{H_2L^H}$ and $\mathbf{H_2L^{NO2}}$ were prepared according to previously reported methods.[24,28] The synthesis for the ligands $\mathbf{H_2L^{Cl}}$, $\mathbf{H_2L^{I}}$, $\mathbf{H_2L^{OMe}}$ and $\mathbf{H_2L^{F}}$ are analogous to the synthesis of the bromo derivative given below and are provided in the ESI†. The synthesis for the complexes $\mathbf{[MoO_2L^{Me}]}$, $\mathbf{[MoO_2L^{Br}]}$, $\mathbf{[MoO_2L^{I}]}$, $\mathbf{[MoO_2L^{NO2}]}$, $\mathbf{[MoO_2L^{OMe}]}$, $\mathbf{[MoO_2L^{F}]}$ and $\mathbf{[MoO_2H_2L^{H}]}$ have been provided in the ESI†.

N,*N*′-dimethyl-*N*,*N*′-*bis*[(5-methyl-2-hydroxyphenyl)methylene]-1,2-diaminoethane ($\mathbf{H_2L^{Me}}$)

To a stirred solution of 2-hydroxy-5-methyl-benzaldehyde (1.00 g, 7.3 mmol) in 20 mL of methanol was slowly added a solution of ethylenediamine (220 mg, 3.7 mmol) in 20 mL of methanol. Upon stirring a yellow precipitate formed and after 30 minutes of stirring, sodium borohydride (556 mg, 14.7 mmol) was added in small portions. When the mixture was colourless, it was poured over 100 mL of water and extracted with dichloromethane to yield a slightly off white powder (934 mg, 86%). The white powder (900 mg, 3.0 mmol) was dissolved in 50 mL of tetrahydrofuran. To this solution was added 10 mL of acetic acid and aqueous formaldehyde (2.84 g, 35 mmol) and the mixture was stirred for 1 hour. Sodium borohydride (574 mg, 15 mmol) was added slowly and the reaction stirred overnight. All volatiles were removed under vacuum and the residue was hydrolysed with sodium hydroxide solution. The aqueous phase was extracted with dichloromethane and the organic phase dried over sodium sulfate. All volatiles were removed under vacuum yielding a white powder (854 mg, 87%). ^{1}H NMR (400 MHz, $CDCl_3$, 298 K): 10.48 (br s, 2H, ArOH), 6.9 (dd, 2H, $^{3}J_{HH} = 8.1$, $^{4}J_{HH} = 1.8$ Hz, ArH), 6.78 (d, 2H, $^{4}J_{HH} = 1.8$, ArH), 6.76 (d, 2H, $^{3}J_{HH} = 8.1$, ArH), 3.68 (s, 4H, NCH_2Ar), 2.68 (s, 4H, $N(CH_2CH_2)N$), 2.30 (s, 6H, NCH_3), 2.26 (s, 2H, $ArCH_3$). ^{13}C NMR (400 MHz, $CDCl_3$, 298 K): 155.37, 129.30, 129.11, 128.20, 121.32, 115.93 (ArC), 61.84, 54.18 (CH_2), 41.77, 20.49 (CH_3). MS (ESI): $m/z = 329$, $[M + H]^+$. Elemental analysis for $C_{20}H_{28}N_2O_2$ (F.W. 328.5): C, 73.14; H, 8.59; N, 8.53%. Found C, 73.03; H, 8.65; N, 8.48%.

N,*N*′-dimethyl-*N*,*N*′-*bis*[(5-bromo-2-hydroxyphenyl)methylene]-1,2-diaminoethane ($\mathbf{H_2L^{Br}}$)

To a stirred mixture of *N*,*N*′-dimethylethylenediamine (1.00 g, 11.3 mmol) and 4-bromophenol (3.93 g, 22.7 mmol) in 50 mL of refluxing methanol was added aqueous formaldehyde (3.68 g, 45.4 mmol). The mixture was refluxed overnight and cooled to room temperature and the white precipitate was filtered off, washed with two portions of cold methanol (2 × 30 mL) and dried under vacuum to yield a white powder (3.28 g, 63%). ^{1}H NMR (400 MHz, $CDCl_3$, 298K): 10.57 (br s, 2H, ArOH), 7.29 (dd, 2H, $^{3}J_{HH} = 8.6$, $^{4}J_{HH} = 2.4$, ArH), 7.09 (d, 2H, $^{4}J_{HH} = 2.4$, ArH), 6.74 (d, 2H, $^{3}J_{HH} = 8.6$, ArH), 3.68 (s, 4H, NCH_2Ar), 2.66 (s, 4H, $N(CH_2CH_2)N$), 2.30 (s, 6H, NCH_3). ^{13}C NMR (400 MHz, $CDCl_3$, 298K): 156.96, 131.74, 131.08, 123.52, 118.11, 110.89 (ArC), 61.27, 53.89 (CH_2), 41.65 (CH_3). MS (ESI): $m/z = 459$, $[M + H]^+$. Elemental analysis for $C_{18}H_{22}Br_2N_2O_2$ (F.W. 458.2): C, 47.18; H, 4.84; N, 6.11%. Found C, 47.26; H, 4.75; N, 6.02%.

$\mathbf{[MoO_2L^H]}$

This compound was prepared in a manner similar to that described previously.[25] To a solution of $\mathbf{H_2L^H}$ (300 mg, 1.0 mmol) in 20 mL acetonitrile was added bis(2,4-pentanedionato)dioxomolybdenum(VI) (326 mg, 1.0 mmol). The reaction mixture was stirred for 6 hours in which time a yellow precipitate formed. The precipitate was filtered and washed with methanol (20 mL) and acetonitrile (20 mL) yielding a yellow powder (303 mg, 71%). ^{1}H NMR (400 MHz, $CDCl_3$, 298K): 7.25 (t, 2H, $^{3}J_{HH} = 7.6$, ArH), 7.05 (d, 2H, $^{3}J_{HH} = 7.6$, ArH), 6.95–6.80 (m, 4H, ArH), 5.10 (d, 2H, $^{2}J_{HH} = 14.3$, $ArCH_2N$), 3.60 (d, 2H, $^{2}J_{HH} = 14.3$, $ArCH_2N$), 3.08 (d, 2H, $^{2}J_{HH} = 9.5$, $(N(CH_2CH_2)N)$), 2.74 (s, 6H, NCH_3), 2.15 (d, 2H, $^{2}J_{HH} = 9.5$, $(N(CH_2CH_2)N)$). ^{13}C NMR (400 MHz, $CDCl_3$, 298K): 159.55, 129.62, 129.42, 122.09, 120.86, 118.70 (ArC), 64.84, 52.01 (CH_2), 48.15 (CH_3). MS (ESI): $m/z = 429$, $[M + H]^+$. Elemental analysis for $C_{18}H_{22}N_2O_4Mo$ (F.W. 426.32): C, 50.71; H, 5.20; N, 6.57%. Found C, 50.82; H, 5.29; N, 6.63%.

$\mathbf{[MoO_2L^{Cl}]}$

This compound was prepared in an analogous manner to that described above for $[MoO_2L^H]$, except $\mathbf{H_2L^{Cl}}$ (369 mg, 1.0 mmol) dissolved in 20 mL of dichloromethane was used in place of $\mathbf{H_2L^H}$ dissolved in acetonitrile to yield an orange powder (345 mg, 70%). ^{1}H NMR (400 MHz, $CDCl_3$, 298K): 7.19 (dd, 2H, $^{3}J_{HH} = 8.7$, $^{4}J_{HH} = 2.5$, ArH), 7.04 (d, 2H, $^{4}J_{HH} = 2.5$, ArH), 6.80 (d, 2H, $^{3}J_{HH} = 8.7$, ArH), 5.02 (d, 2H, $^{2}J_{HH} = 14.5$, $ArCH_2N$), 3.55 (d, 2H, $^{2}J_{HH} = 14.5$, $ArCH_2N$), 3.03 (d, 2H, $^{2}J_{HH} = 9.7$, $(N(CH_2CH_2)N)$), 2.71 (s, 6H, NCH_3), 2.19 (d, 2H, $^{2}J_{HH} = 9.7$, $(N(CH_2CH_2)N)$). ^{13}C NMR (400 MHz, $CDCl_3$, 298K): 158.17,

129.34, 129.20, 125.41, 123.42, 120.05 (ArC), 64.22, 52.07 (CH_2), 48.08 (CH_3). MS (ESI): $m/z = 497$, $[M + H]^+$. Elemental analysis for $C_{18}H_{20}Cl_2N_2O_4Mo$ (F.W. 495.2): C, 43.66; H, 4.07; N, 5.66%. Found C, 43.70; H, 4.13; N, 5.73%.

X-Ray crystallography

Crystals of **$[MoO_2L^{Cl}]$** suitable for X-ray diffraction were grown from chloroform by slow evaporation of the solvent. Crystal data for $[MoO_2L^{Cl}]$: $C_{18}H_{20}Cl_2MoN_2O_4$, $M = 495.20$, monoclinic, $I2/a$ (no. 15), $a = 14.45109(12)$, $b = 7.45243(6)$, $c = 18.62581(17)$ Å, $\beta = 98.5896(8)°$, $V = 1983.42(12)$ Å^3, $Z = 4$ [C_2 symmetry], $D_c = 1.658$ g cm^{-3}, μ(Cu–Kα) = 8.122 mm^{-1}, $T = 173$ K, yellow plates, Oxford Diffraction Xcalibur PX Ultra diffractometer; 1894 independent measured reflections ($R_{int} = 0.0214$), F^2 refinement, R_1(obs) = 0.021, wR_2(all) = 0.060, 1757 independent observed absorption-corrected reflections [$|F_o| > 4\sigma(|F_o|)$, $2\theta_{max} = 143°$], 123 parameters. The structure was solved and refined using the SHELXTL (PC version 5.1, Bruker AXS, Madison, WI, 1997) and SHELX-97 (G. Sheldrick, Institut Anorg. Chemie, Tammannstr. 4, D37077 Göttingen, Germany, 1998) software packages. CCDC 689173. Further details may be found in the ESI.†

Oxidation reactions

Two different experimental procedures were used for the oxidation of PPh_3:

Procedure A. (used for the Hammett analysis): To the catalyst **$[MoO_2L^x]$** (0.025 mmol) and 0.25 mmol (10 equivalents) of PPh_3 was added 5 mL of DMSO at room temperature and the mixture was stirred vigorously for 2 minutes to ensure complete dissolution. An aliquot of the reaction solution was placed in the NMR Spectrometer, which had been pre-heated to 130 °C. A spectrum was obtained every 3 minutes for 6 hours (apart from **$[MoO_2L^{NO2}]$** where, due to the fast rate of the reaction, a spectrum was obtained every minute). A representative example is shown in Fig. 2.

Procedure B. (used to determine the rate equation for **$[MoO_2L^{NO2}]$**): Triphenylphosphine (2.5 mmol) was placed in an ampoule and oxidised in 5 mL dimethylsulfoxide in the presence of an amount of catalyst and aliquots removed from the bulk at 30, 60, 90, 120 and 150 minutes. These samples were mixed with 25% v/v of $CDCl_3$ and analysed by ^{31}P NMR spectroscopy.

Cyclic voltammetry

The complex **$[MoO_2L^X]$** (20 mg, ca. 0.05 mmol) was dissolved in 50 mL of a 0.2 M solution of NBu_4PF_6 in DMF. Part of this solution was transferred to an electrochemical cell. The data for cyclic voltammograms (3 scans) at scan rates of 50, 100 and 200 mV s^{-1} were collected. Individual scans can be found in the ESI†.

Results and discussion

Ligand and complex synthesis

The unsubstituted salan ligands **H_4L^H** and **H_2L^H** were prepared as previously described.[28] Condensation of ethylenediamine with salicylaldehyde followed by a reduction with sodium borohydride to yield **H_4L^H** and subsequent methylation of the amine to yield **H_2L^H** is shown in eqn (1). It was also possible to synthesise **H_2L^{Me}** by this method, but not the other ligands.

Ortho/*para*-disubstituted salan ligands are generally prepared by a Mannich condensation reaction.[29] Kerton and co-workers have reported the synthesis of a salan ligand with no *ortho*-substituents (**H_2L^{Me}**) *via* a Mannich condensation reaction,[30] but this method failed in our hands for this particular ligand. However, the Mannich condensation protocol was successfully employed for the synthesis of **H_2L^F**, **H_2L^I**, **H_2L^{Br}**, **H_2L^{Cl}** and **H_2L^{OMe}** (eqn (2)). It was not possible to synthesise **H_2L^{NO2}** by any of the routes shown in eqn (1) and (2). Instead, it was necessary to react 2-(chloromethyl)-4-nitrophenol with *N*,*N*′-dimethylethylenediamine (eqn (3)) as described previously by Ng.[24]

The complexes were prepared by reaction of the ligand with $[MoO_2(acac)_2]$ in methanol and a solvent system in which the ligand dissolves, typically acetonitrile or a mixture of

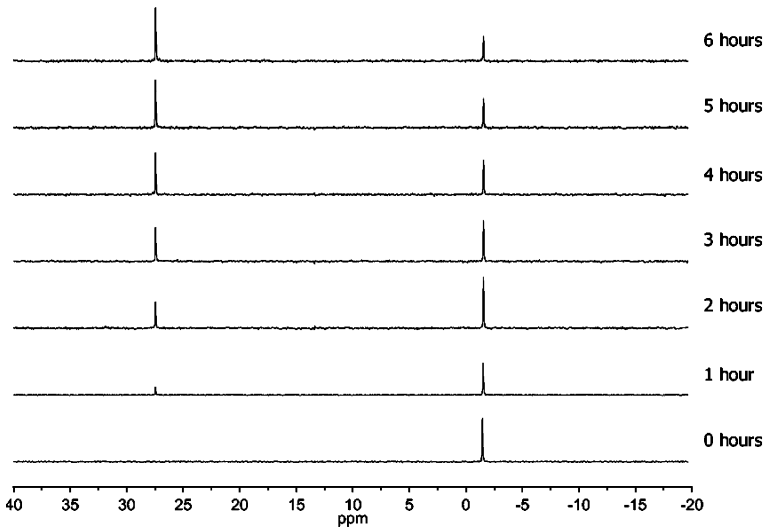

Fig. 2 A series of ^{31}P NMR spectra for the reaction between PPh3 and DMSO at 130 °C, catalysed by **$[MoO_2L^{Cl}]$** according to procedure A.

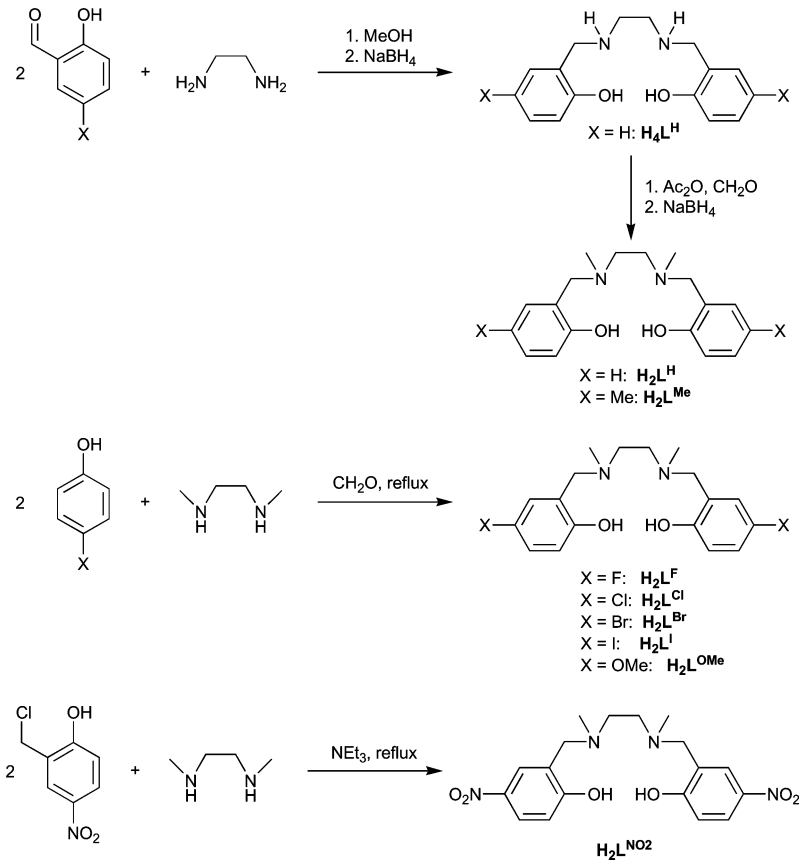

(1)

(2)

(3)

dichloromethane and acetonitrile. This gave yellow or orange complexes in moderate to good yields, which did not require any further purification. All ligands and subsequent complexes have been characterised by ^{1}H, ^{13}C and where applicable ^{19}F NMR spectroscopy as well as mass spectrometry and elemental analysis. In the case of **[MoO$_2$L^{Cl}]**, crystals suitable for X-ray analysis were obtained from chloroform by slow evaporation of the solvent. Fig. 3 shows the molecular structure of **[MoO$_2$L^{Cl}]** along with selected bond lengths and angles in Table 1. The complex has crystallographic C_2 symmetry about an axis which passes through the molybdenum and bisects the C9–C9′ bond and the ligand has adopted a *cis*-α (*R**,*R**) topology, whereby *R** refers to the relative configuration at the amine nitrogen atoms. ^{1}H NMR analysis and in particular the ^{19}F NMR spectrum of the related complex **[MoO$_2$L^{F}]**, which contains only a single resonance at −121 ppm, indicate that this is also the only geometry observed in solution. Bond lengths and angles are unremarkable and comparable to similar Mo(VI) dioxo complexes containing salan type ligands.[21,22,25,31]

Table 1 Selected bond lengths (Å) and angles (°) for **[MoO$_2$L^{Cl}]**

Mo–O	1.7035(15)	Mo–O(1)	1.9381(14)
Mo–N(8)	2.3945(19)		
O–Mo–O(1)	96.54(6)	O–Mo–N(8)	163.55(8)
O–Mo–O′	108.17(11)	O–Mo–O(1′)	97.56(7)
O–Mo–N(8′)	88.24(7)	O(1)–Mo–N(8)	79.69(6)
O(1)–Mo–O(1′)	155.86(9)	O(1)–Mo–N(8′)	81.26(6)
N(8)–Mo–N(8′)	75.39(10)		

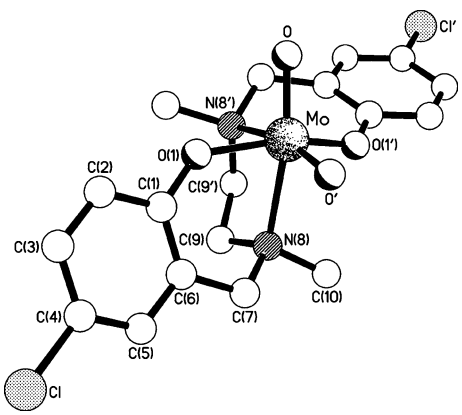

Fig. 3 The molecular structure of **[MoO$_2$L^{Cl}]**.

Triphenylphosphine oxidation studies

The ability of molybdenum(VI) *cis*-dioxo complexes to catalyse oxo-transfer reactions has been investigated using PPh_3 as the substrate and DMSO as the oxygen transfer agent (for details see Experimental). The decrease of the concentration of PPh_3 was monitored over time (see Fig. 2) for all Mo(VI) complexes and from the data shown in Fig. 4, where $\ln[PPh_3]/[PPh_3]_0$ is plotted against time, it can be seen that all reactions are first order with respect to the triphenylphosphine concentration. An important outcome of this study is that the rate of oxidation of PPh_3 appears to be directly related to the electron-withdrawing ability of the *para* phenoxy substituent on the molybdenum catalyst.

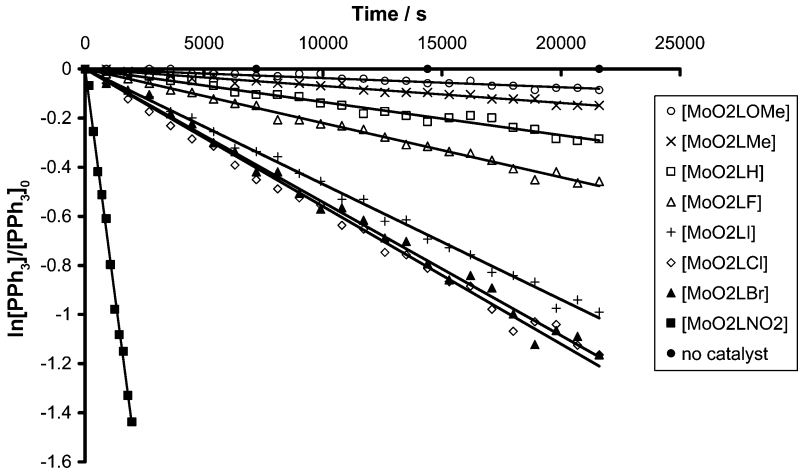

Fig. 4 Variation in [PPh_3] *versus* time in the catalysed oxo transfer reaction between DMSO and PPh_3. Conditions: $[PPh_3]_0$ = 50 mM (10 equiv.); [catalyst] = 5 mM (1 equiv) in DMSO at 130 °C.

Hammett parameters allow the quantification of the effect of electron-donating and electron-withdrawing substituents on the outcome of a reaction and this can give important insight into the mechanism of the reaction.[32] For example, Holm and Sung have applied Hammett parameters in a related mechanistic study of the oxo transfer process catalysed by bis(dithiolene) tungsten complexes.[33] Previous studies on oxidation reactions with molybdenum(VI) *cis*-dioxo complexes as catalysts featured salan ligands with both *ortho*- and *para*-substituted phenoxy groups.[23–25] This double substitution precludes the use Hammett parameters, as both substituents will affect the catalytic activity and the *ortho* substituent will have an additional steric effect. In order to gain further insight into the mechanism of oxygen transfer catalysed by salan molybdenum dioxo complexes we have applied Hammett analysis to the *para*-substituted complexes studied here.

The kinetic data obtained in Fig. 4 have been used to construct a Hammett diagram, as shown in Fig. 5. The straight line (R^2 = 0.986) and the gradient (ρ value) of 2.2 indicate the accumulation of negative charge during the rate-determining step in the catalytic cycle. These observations are consistent with the previously proposed mechanism involving nucleophilic attack by the phosphine at an oxo ligand.[10,34,35] In several related molybdenum-based systems, this nucleophilic attack has been identified as the rate determining step in the oxygen atom transfer process.[8,36] From the Hammett analysis shown in Fig. 5, it can be concluded that this is also the case here, whereby the nucleophilic attack results in a charge build-up at the molybdenum centre. Electron-withdrawing substituents will lower the energy of the transition state by dissipating the negative charge, which results in faster reaction rates.

Catalyst decompostion

Previous studies have shown that during oxygen atom transfer catalysis, a potential deactivation pathway for the molybdenum catalysts is the comproportionation reaction between Mo(VI) dioxo and Mo(IV) oxo complexes to give oxo-bridged dimeric Mo(V) complexes (eqn (4)).[22,37–39] Once formed, these dimeric complexes are rather stable and can no longer participate in further catalytic turnover. If the order of reaction with respect to catalyst

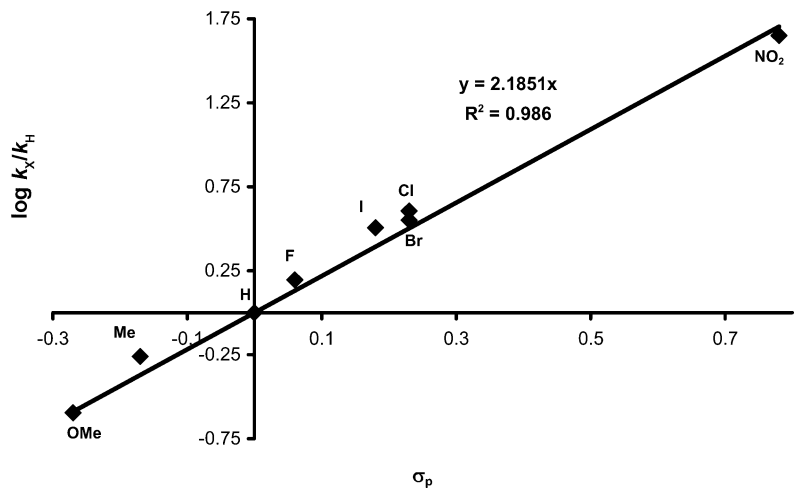

Fig. 5 Relative rate constants log k_X/k_H *versus* the Hammett σ_p parameter for the oxo transfer reaction between DMSO and PPh_3, catalysed by salan Mo complexes.

substantially deviates from the expected first order, it is plausible that the deviation is caused by the formation of inactive oxo-bridged Mo(v) complexes. In order to investigate this potential catalyst deactivation pathway, the conversion of PPh_3 to Ph_3PO was monitored using different concentrations of the most active catalyst **[MoO_2L^{NO2}]**.

Using the integrated rate law (as shown in Fig. 4) it was possible to assign the rate equation as first order with respect to PPh_3 concentration. Using eqn (5)–(7) and the relationship between $\ln k_{app}$ and ln[catalyst], as shown in Fig. 6, it can be seen that the rate order with respect to catalyst concentration is approximately unity (x = 1.0128) and hence formation of inactive dimeric oxo-bridged Mo(v) complexes either does not occur or the formation is fast and reversible. The rate constant for the oxygen transfer reaction between Me_2SO and PPh_3 by the most active catalyst **[MoO_2L^{NO2}]** at 130 °C was determined as $k_0 = 7.13 \times 10^{-2}$ L mol^{-1} s^{-1}. The rate equation shown in eqn (8) is the same as the one determined previously for the reaction of $EtPPh_2$ with dioxomolybdenum(vi) complexes containing tridentate Schiff base ligands,[16] which confirms that the rate determining step is indeed the initial reaction of the phosphine and the dioxo complex.

$$[LMo^{VI}O_2] + [LMo^{IV}O] \longrightarrow LMo^{V}(=O)-O-Mo^{V}(=O)L \quad (4)$$

$$\text{rate} = k_{app}[PPh_3] \quad (5)$$

$$k_{app} = k_0\,[MoO_2L^{NO2}]^x \quad (6)$$

$$\ln k_{app} = \ln k_0 + x\ln[MoO_2L^{NO2}] \quad (7)$$

$$\text{rate} = k_0[PPh_3][MoO_2L^{NO2}] \quad (8)$$

Cyclic voltammetry studies

The electrochemical properties of the salan molybdenum dioxo complexes **[MoO_2L^X]** used in the oxo transfer experiments, together with the complex which contains a secondary amine ligand **[$MoO_2(H_2L^H)$]**, have been investigated in DMF. The cyclic voltammograms exhibit a single quasi-reversible peak for most complexes, with $E_{1/2}$ values ranging from –1.097 V for **[MoO_2L^I]** to –1.271 V for **[MoO_2L^{OMe}]** (see Table 2), which correspond to a reduction from Mo(vi) to Mo(v) complexes (eqn (9)). These values indicate that these salan dioxomolybdenum complexes are slightly easier to reduce than the related bis(phenoxy)diamine complexes reported by Ng.[23] The cyclic voltammogram of **[MoO_2L^{NO2}]**, shown in Fig. 7, displays an additional quasi-reversible electron transfer couple. This peak is assigned to a further reduction of Mo(v) to Mo(iv) (eqn (10)). The electron-withdrawing *para*-nitro substituents lower the reduction potential to such an extent that further reduction to Mo(iv) becomes accessible. This second reduction is not observed with any of the other complexes, in which case reduction of the DMF solvent takes place before any further reduction to Mo(iv) can occur. Another exception is complex **[$MoO_2(H_2L^H)$]**, which displays irreversible electrochemical reduction behaviour. Similar observations were made previously by Spence and co-workers[22] and this was attributed to ligand oxidation (eqn (11)).

Table 2 Half potentials for Mo(vi)/Mo(v) redox couples in salan molybdenum dioxo complexes

Complex	$E_{1/2}$/V *vs.* Ag/AgCl
[$MoO_2(H_2L^H)$]	Irreversible
[MoO_2L^{OMe}]	–1.271
[MoO_2L^{Me}]	–1.255
[MoO_2L^H]	–1.206
[MoO_2L^F]	–1.177
[MoO_2L^{Cl}]	–1.111
[MoO_2L^{Br}]	–1.112
[MoO_2L^I]	–1.097
[MoO_2L^{NO2}]	–0.803, –1.304 (Mo(v)/Mo(iv))

The half-potential values $E_{1/2}$ for the Mo(vi)/Mo(v) redox couple have been plotted against the Hammett σ_p values for the *para* substituents as shown in Fig. 8. A linear relationship between the $E_{1/2}$ values and the Hammett parameter is observed, which indicates that the substituents in the *para* phenoxy position directly affect the electron density at the molybdenum centre. A linear relationship has been previously observed for molybdenum dioxo complexes containing tridentate Schiff base ligands.[18]

The correlation between the $E_{1/2}$ values and the catalytic oxo transfer activity indicates that the variation in catalytic activity is directly related to electronic effects at the metal centre. Steric effects do not appear to be involved in this series of *para*-phenoxy

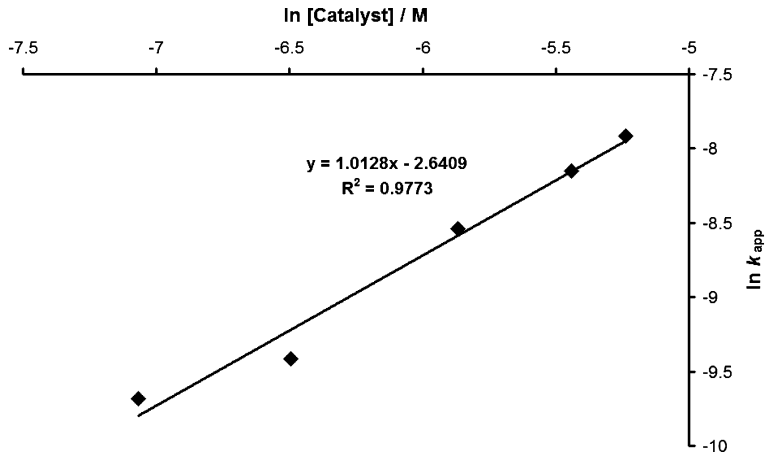

Fig. 6 The relation ship between $\ln k_{app}$ and ln[catalyst] for the oxo transfer reaction between DMSO and PPh_3, catalysed by salan Mo complexes.

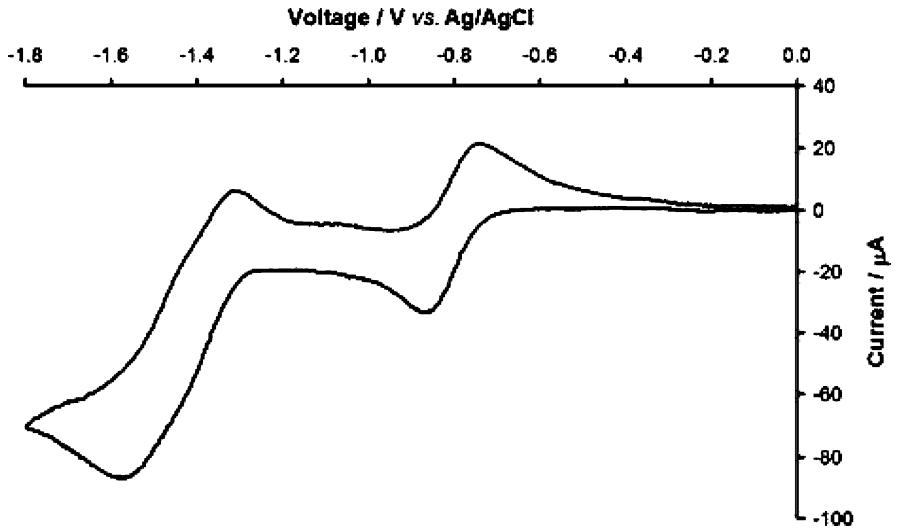

Fig. 7 Cyclic voltammogram of $[MoO_2L^{NO2}]$. Conditions: room temperature in DMF, [complex] = 1 mM; $[NBu_4PF_6]$ = 0.2 M; scan speed 100 mV s^{-1}; working electrode, Pt stick; auxilliary electrode, Pt wire; reference electrode, Ag/AgCl.

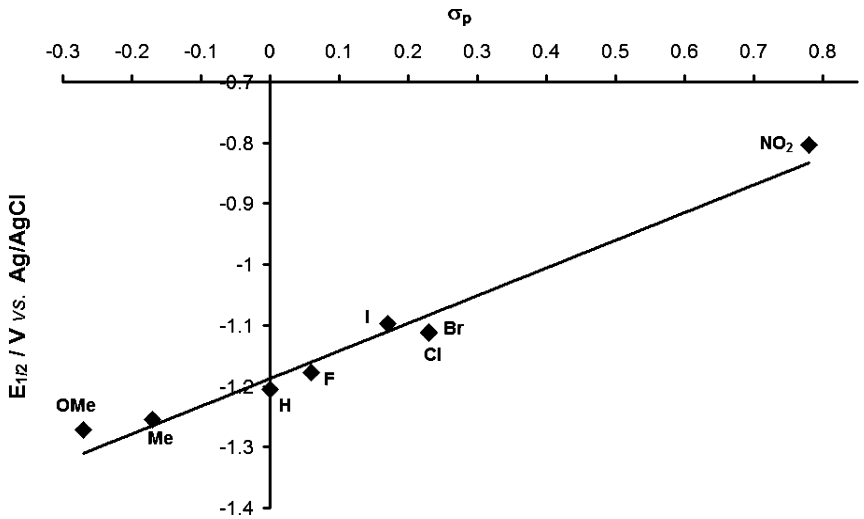

Fig. 8 Relationship between $E_{1/2}$ values for the Mo(VI)/Mo(V) redox couple and the Hammett values σ_p. Conditions: room temperature, DMF, [complex] = 1 mM, $[NBu_4PF_6]$ = 0.2 M; scan speed 100 mV s^{-1}; working electrode, Pt stick; auxiliary electrode, Pt wire; reference electrode, Ag/AgCl.

substituted catalysts, but they will become important with *ortho*-phenoxy substitution, which will be the subject of future studies. Interestingly, a similar relationship has been previously observed in alkene epoxidation catalysed by related salen manganese complexes.[40]

$$\left[MoO_2\left(L^X\right)\right] \xrightarrow{e^-} \left[MoO_2\left(L^X\right)\right]^- \quad (9)$$

$$\left[MoO_2\left(L^X\right)\right]^- \xrightarrow{e^-} \left[MoO_2\left(L^X\right)\right]^{2-} \quad (10)$$

$$\left[MoO_2\left(H_2L^H\right)\right] \xrightarrow{e^-} \left[MoO_2\left(L^H\right)\right]^- + H_2O \quad (11)$$

Mechanistic implications

The positive slope in the Hammett analysis in Fig. 5 has shown that in the catalytic oxygen transfer reaction between DMSO and PPh_3, a negative charge must build up during the rate-determining step in the catalytic cycle. These observations are consistent with the mechanism shown in Scheme 1, which was first proposed by Holm and co-workers.[41] Computational studies have complemented these kinetic studies and oxo atom transfer processes are currently believed to go through two transition states, one involving the formation of a phosphine oxide intermediate and one involving a substitution reaction, which leads to product release.[10] The first reaction involves nucleophilic attack by the phosphine at the oxygen atom, specifically attack of P on the Mo=O π^* orbital, to give a phosphine oxide intermediate.[8] Intermediates of this type have been isolated recently for complexes of the type [LMo(IV)O(OPR_3)X], where L = hydrotris(3-isopropylpyrazolyl-1-yl)borate (Tp^{iPr}) and X = Cl^-, phenolates, thiolates),[8,9,41,42] and where L = hydrotris(3,5-dimethylpyrazol-1-yl)borate (Tp*) and X = Cl^-.[10,43] The next step involves a substitution at the octahedral d^2 Mo(IV) intermediate which, based on previous theoretical studies,[34] was described as an associative or associative interchange (I_a) process in the case of displacement of OPR_3 by H_2O. However,

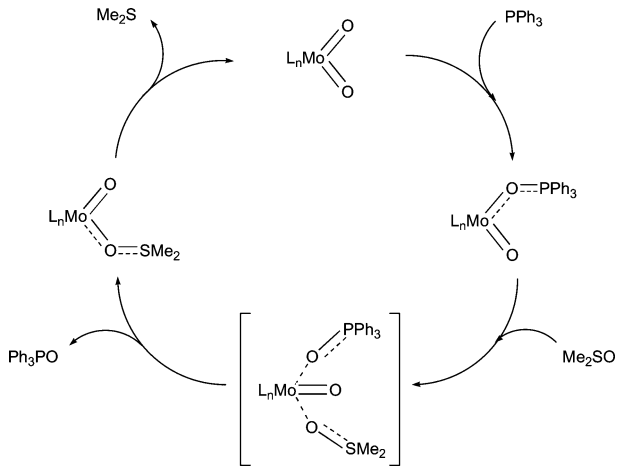

Scheme 1

recent theoretical studies on the displacement of OPR_3 by CH_3CN, suggest a dissociative or dissociative-interchange (I_d) mechanism for this reaction.[8] More studies are clearly needed to unravel all aspects of the mechanism of this intriguing oxo transfer process.

In summary, we have prepared a series of *para*-substituted salan ligands and their corresponding Mo(VI) dioxo complexes and we have evaluated their ability to catalyse the oxo transfer reaction between triphenylphosphine and dimethylsulfoxide. The relative rate constants have been plotted against Hammett σ_p parameters and it has been shown that the rate-determining step involves a nucleophilic attack of the lone pair of the phosphorus atom at the oxo ligand. We have also shown that, at least for the most active *para*-nitro substituted catalyst, the formation of inactive oxo-bridged dimeric Mo(V) complexes does not appear to occur. Electrochemical studies have shown that $E_{1/2}$ and Hammett σ_p parameters can be correlated for these complexes and that all the complexes exhibit quasi-reversible redox behaviour. These studies have shown that electron withdrawing substituents can be used to increase the catalytic activity of salan molybdenum dioxo catalysts and in future studies we will apply these findings for the development of catalysts for the oxidation of more challenging substrates such as alkenes with cheaper and more environmentally friendly oxidants such as O_2 or H_2O_2.

Acknowledgements

We gratefully acknowledge financial support from the Department of Chemistry, Imperial College, London. We are grateful to Peter Haycock and Richard Sheppard for their assistance in kinetic NMR measurements.

References

1 J. M. Tunney, J. McMaster and C. D. Garner, *Comp. Coord. Chem. II*, 2004, **8**, 459.
2 R. Hille, *Chem. Rev.*, 1996, **96**, 2757.
3 J. H. Enemark, J. J. A. Cooney, J.-J. Wang and R. H. Holm, *Chem. Rev.*, 2004, **104**, 1175.
4 J. McMaster, J. M. Tunney and C. D. Garner, *Prog. Inorg. Chem.*, 2003, **52**, 539.
5 C. G. Young, in '*Biomimetic Oxidations Catalyzed by Transition Metal Complexes*', ed. B. Meunier, Imperial College Press, London, 2000, pp. 415.
6 J. M. Berg and R. H. Holm, *J. Am. Chem. Soc.*, 1985, **107**, 917.
7 J. M. Berg and R. H. Holm, *J. Am. Chem. Soc.*, 1985, **107**, 925.
8 B. W. Kail, L. M. Pérez, S. D. Zaric, A. J. Millar, C. G. Young, M. B. Hall and P. Basu, *Chem.–Eur. J.*, 2006, **12**, 7501.
9 A. J. Millar, C. J. Doonan, P. D. Smith, V. N. Nemykin, P. Basu and C. G. Young, *Chem.–Eur. J.*, 2005, **11**, 3255.
10 V. N. Nemykin and P. Basu, *Inorg. Chem.*, 2005, **44**, 7494.
11 Z. Xiao, M. Bruck, C. Doyle, J. H. Enemark, C. Grittini, R. W. Gable, A. G. Wedd and C. G. Young, *Inorg. Chem.*, 1995, **34**, 5950.
12 Z. Xiao, M. A. Bruck, J. H. Enemark, C. G. Young and A. G. Wedd, *Inorg. Chem.*, 1996, **35**, 7508.
13 Z. Xiao, C. G. Young, J. H. Enemark and A. G. Wedd, *J. Am. Chem. Soc.*, 1992, **114**, 9194.
14 G. Lyashenko, G. Saischeck, A. Pal, R. Herbst-Irmer and N. C. Mösch-Zanetti, *Chem. Commun.*, 2007, 701.
15 J. Topich and J. T. Lyon III, *Inorg. Chim. Acta*, 1983, **80**, L41.
16 J. Topich and J. T. Lyon III, *Polyhedron*, 1984, **3**, 61.
17 J. Topich and J. T. Lyon III, *Inorg. Chem.*, 1984, **23**, 3202.
18 J. Topich and J. T. Lyon III, *Polyhedron*, 1984, **3**, 55.
19 O. A. Rajan, J. T. Spence, C. Leman, M. Minelli, M. Sato, J. H. Enemark, P. M. H. Kroneck and K. Sulger, *Inorg. Chem.*, 1983, **22**, 3065.
20 D. Dowerah, J. T. Spence, R. Singh, A. G. Wedd, G. L. Wilson, F. Farchione, J. H. Enemark, J. Kristofzski and M. Bruck, *J. Am. Chem. Soc.*, 1987, **109**, 5655.
21 C. J. Hinshaw, G. Peng, R. Singh, J. T. Spence, J. H. Enemark, M. Bruck, J. Kristofzski, S. L. Merbs, R. Ortega and P. A. Wexler, *Inorg. Chem.*, 1989, **28**, 4483.
22 P. Subramanian, J. T. Spence, R. Ortega and J. H. Enemark, *Inorg. Chem.*, 1984, **23**, 2564.
23 Y.-L. Wong, J.-F. Ma, W.-F. Law, Y. Yan, W.-T. Wong, Z.-Y. Zhang, T. C. W. Mak and D. K. P. Ng, *Eur. J. Inorg. Chem.*, 1999, 313.
24 Y.-L. Wong, Y. Yan, E. S. H. Chan, Q. Yang, T. C. W. Mak and D. K. P. Ng, *J. Chem. Soc., Dalton Trans.*, 1998, 3057.
25 A. Lehtonen and R. Sillanpää, *Polyhedron*, 2005, **24**, 257.
26 R. H. Holm and J. P. Donahue, *Polyhedron*, 1993, **12**, 571.
27 B. Soptrajanov, A. Nikolovski and I. Petrov, *Spectrochim. Acta*, 1968, **24A**, 1617.
28 J. Balsells, P. J. Carroll and P. J. Walsh, *Inorg. Chem.*, 2001, **40**, 5568.
29 E. Y. Tshuva, N. Gendeziuk and M. Kol, *Tetrahedron Lett.*, 2001, **42**, 6405.
30 F. M. Kerton, A. C. Whitwood and C. E. Willans, *Dalton Trans.*, 2004, 2237.
31 H. Elias, F. Stock and C. Röhr, *Acta Crystallogr.*, 1997, **C53**, 862.
32 C. Hansch, A. Leo and R. W. Taft, *Chem. Rev.*, 1991, **91**, 165.
33 K.-M. Sung and R. H. Holm, *J. Am. Chem. Soc.*, 2002, **124**, 4312.
34 M. A. Pietsch and M. B. Hall, *Inorg. Chem.*, 1996, **35**, 1273.
35 S. B. Seymore and S. N. Brown, *Inorg. Chem.*, 2000, **39**, 325.
36 K. Heinze and A. Fisher, *Eur. J. Inorg. Chem.*, 2007, 1020.
37 J. A. Craig, E. W. Harlan, B. S. Snyder, M. A. Whitener and R. H. Holm, *Inorg. Chem.*, 1989, **28**, 2082.
38 C. J. Doonan, D. A. Slizys and C. G. Young, *J. Am. Chem. Soc.*, 1999, **121**, 6430.
39 L. Stelzig, S. Kötte and B. Krebs, *J. Chem. Soc., Dalton Trans.*, 1998, 2921.
40 M. Palucki, N. S. Finney, P. J. Pospisil, M. L. Guler, T. Ishida and E. N. Jacobsen, *J. Am. Chem. Soc.*, 1998, **120**, 948.
41 C. J. Doonan, A. J. Millar, D. J. Nielsen and C. G. Young, *Inorg. Chem.*, 2005, **44**, 4506.
42 P. D. Smith, A. J. Millar, C. G. Young, A. Ghosh and P. Basu, *J. Am. Chem. Soc.*, 2000, **122**, 9298.
43 V. N. Nemykin, J. Laskin and P. Basu, *J. Am. Chem. Soc.*, 2004, **126**, 8604.

